PHILOSOPHICAL TRANSACTIONS OF THE ROYAL SOCIETY A MATHEMATICAL, PHYSICAL & ENGINEERING SCIENCES

Charge Storage and Charge Transport in Conducting Polymers: Solitons, Polarons and Bipolarons [and Discussion]

A. J. Heeger and R. Pethig

Phil. Trans. R. Soc. Lond. A 1985 **314**, 17-35
doi: 10.1098/rsta.1985.0005

Phil. Trans. R. Soc. Lond. A **314**, 17–35 (1985) [17]
Printed in Great Britain

Charge storage and charge transport in conducting polymers: solitons, polarons and bipolarons

By A. J. Heeger

Institute for Polymers and Organic Solids, University of California, Santa Barbara, California 93106, *U.S.A.*

The results of a series of experiments demonstrate that solitons are the important excitations in *trans*-$(CH)_x$ and that the properties of these nonlinear excitations can be directly studied during photoexcitation or after doping. The importance of these concepts in the more general context of conducting polymers is addressed. Although the twofold degenerate ground state of *trans*-$(CH)_x$ is quite special, the relevant concepts have been generalized to confined soliton pairs (bipolarons). Experimental results that demonstrate electron–hole symmetry and weak confinement in polythiophene make this polyheterocycle a nearly ideal example of a model system in which the ground-state degeneracy has been lifted. In the dilute doping régime, *in situ* absorption spectroscopy data (during electrochemical doping) strongly suggest charge storage via bipolarons with confinement parameter $\gamma \approx 0.1$–0.2. These results on polythiophene demonstrate that a quantitative fundamental understanding is possible even for relatively complex systems.

I. Introduction

In traditional three-dimensional semiconductors, the fourfold (or sixfold, etc.) coordination of each atom to its neighbour through covalent bonds leads to a rigid structure. In such systems, therefore, the electronic excitations can usually be considered in the context of this rigid structure leading to the conventional concepts of electrons and holes as the dominant excitations. The situation in semiconductor polymers is quite different; the twofold coordination makes these systems generally more susceptible to structural distortion. As a result, the dominant 'electronic' excitations are inherently coupled to chain distortions. Thus, quite generally, one expects that solitons, polarons, and bipolarons will be the excitations of major importance in this class of one-dimensional polymer semiconductors. We illustrate these concepts in this paper through a summary of experimental results on two systems;

(i) polyacetylene, $(CH)_x$, where the degenerate ground state leads to solitons as the important excitations and the dominant charge storage species;

(ii) polythiophene, where the ground-state degeneracy is lifted so that polarons and bipolarons are the important excitations with charge storage in bipolarons.

As shown in figure 1, *trans*-$(CH)_x$ is a twofold degenerate Peierls insulator that allows for the possibility of nonlinear excitations in the form of soliton-like bond alternation domain walls, each with an associated electronic state at the centre of the energy gap (Heeger 1981*a*; Su *et al.* 1979, 1980*a*; Rice 1979; Takayama *et al.* 1980; Brazovskii 1979, 1980; Brazovskii *et al.* 1981). For polythiophene, on the other hand, the two structures sketched in figure 2 are not energetically equivalent. Polythiophene (PT) can be viewed as an sp^2p_z carbon chain in a

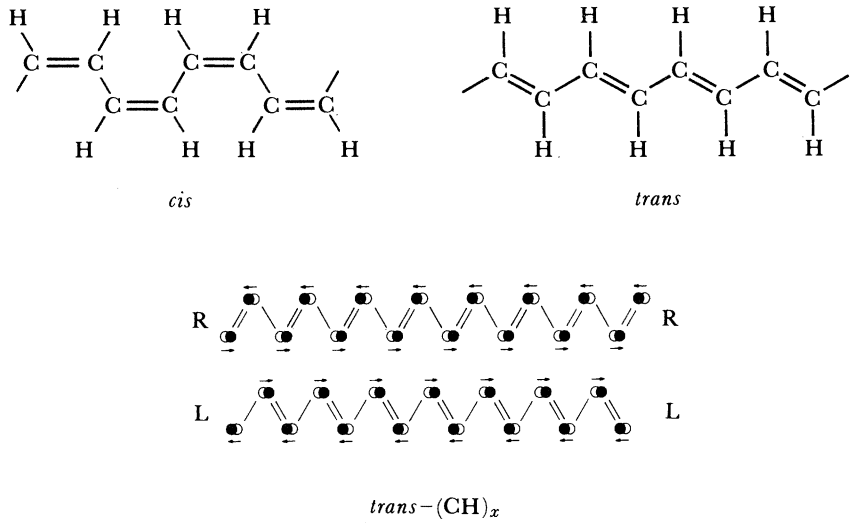

FIGURE 1. (*a*) The chemical structures of *cis*-$(CH)_x$ and *trans*-$(CH)_x$. (*b*) The two degenerate ground-state structures of *trans*-$(CH)_x$. The atomic distortions are indicated by the arrows.

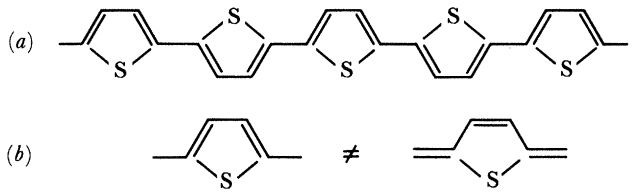

FIGURE 2. (*a*) Chemical structure of polythiophene. (*b*) Two inequivalent structures for the thiophene heterocycle in polythiophene.

structure analogous to that of *cis*-$(CH)_x$, but stabilized in that structure by the sulphur, which covalently bonds to neighbouring carbon atoms to form the heterocycle.

In this paper, we briefly summarize the results of a series of experiments that demonstrate that solitons are important excitations in *trans*-$(CH)_x$, and that the properties of these nonlinear excitations can be directly studied through measurements on *trans*-$(CH)_x$ samples either during photoexcitation or after doping. Having established the relevance of these coupled electronic lattice excitations in *trans*-$(CH)_x$, the importance of these concepts in the more general context of conducting polymers is addressed. Although the twofold degenerate ground state of *trans*-$(CH)_x$ is quite special, the relevant concepts can be generalized to confined soliton pairs (bipolarons) and applied to a wide variety of conjugated polymers in which the ground-state degeneracy is not present. Experimental results that demonstrate electron–hole symmetry and weak confinement in polythiophene make this polyheterocycle a nearly ideal example of a model system in which the ground-state degeneracy has been lifted.

II. SOLITONS AND BIPOLARONS: SOME CONCEPTS

The soliton in $(CH)_x$ is a topological kink in the electron–lattice system; a bond alternation domain wall connecting the two phases with opposite bond alternation. Because there is translational symmetry (the kink can be anywhere) and the mass is small, the soliton should

be mobile. The competition of elastic and condensation energies spreads the domain wall over a region of about 12–14a, where a is the C–C distance along the $(CH)_x$ chain. Although single soliton defects can exist on imperfect chains (and have been studied extensively; see Weinberger *et al.* 1980; Nechtschein *et al.* 1980), intrinsic excitations, either photoproduced or doping-induced, must occur in the form of soliton–antisoliton (S–$\bar{S}$) pairs.

Associated with the structural kink is a localized electronic state with energy at mid-gap (see figure 3a). This electronic state is a solution of the Schrödinger equation in the presence of

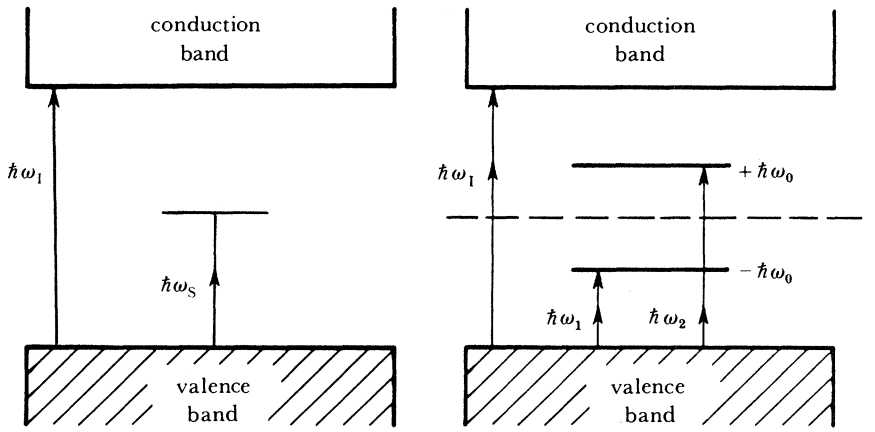

FIGURE 3. (a) Energy level diagram for a charged (positive) soliton in *trans*-$(CH)_x$. The allowed transitions are at $\hbar\omega_1 = 2\Delta$ (interband) and $\hbar\omega_S = \Delta$ (soliton mid-gap transition). (b) Energy level diagram for a charged (positive) bipolaron. Because of the splitting of the levels there are two possible transitions in addition to $\hbar\omega_1$.

the structural domain wall and can therefore accommodate 0, 1, or 2 electrons (Heeger 1981a; Su *et al.* 1979, 1980a; Rice 1979; Takayama *et al.* 1980; Brazovskii 1979, 1980; Brazovskii *et al.* 1981). The neutral soliton has one electron in the mid-gap state and the positively and negatively charged solitons have zero or two electrons respectively in the mid-gap state. Consequently, the spin–charge relations of solitons are reversed; charged solitons are non-magnetic, whereas a neutral soliton has spin $\frac{1}{2}$. The reversed spin–charge relationship for solitons in *trans*-$(CH)_x$ is a direct manifestation of charge fractionalization discovered in the mathematical analysis of spinless fermion systems (Jackliw *et al.* 1979, 1981). In *trans*-$(CH)_x$, the localized mid-gap state of the soliton derives from one half a state removed from the occupied valence band and one half a state from the empty conduction band for each sign of spin. Thus, although the charge fractionalization is masked by the spin degeneracy in *trans*-$(CH)_x$, the resulting reversed spin–charge relation has the same physical origin.

Theoretical analysis (Su *et al.* 1979, 1980a; Rice 1979; Takayama *et al.* 1980; Brazovskii 1979, 1980; Brazovskii *et al.* 1981) has demonstrated that a charged soliton represents the lowest energy configuration for an excess charge on a *trans*-$(CH)_x$ chain; i.e. $E_S < \Delta$ where E_S is the energy for creation of a soliton and Δ is the energy for creation of an electron or hole, $\Delta = E_g/2$. Both numerical calculations using a discrete lattice model (Su *et al.* 1979, 1980a), and analytical results for a continuum model (Takayama *et al.* 1980; Brazovskii 1979, 1980; Brazovskii *et al.* 1981) indicate that (neglecting electron–electron Coulomb interaction)

$$2E_S = (4/\pi)\,\Delta. \tag{1}$$

PHILOSOPHICAL TRANSACTIONS OF THE ROYAL SOCIETY A MATHEMATICAL, PHYSICAL & ENGINEERING SCIENCES

Charged solitons are therefore formed by electron transfer on to or off the polymer chains on doping with electron donors or acceptors.

An analogy can be constructed (Chung *et al.* 1984) between PT and $(CH)_x$ as shown in the diagrams of figure 4 where we redraw the polythiophene backbone structure, purposely leaving out the sulphur heteroatom. The resulting structure is that of an sp^2p_z polyene chain consisting

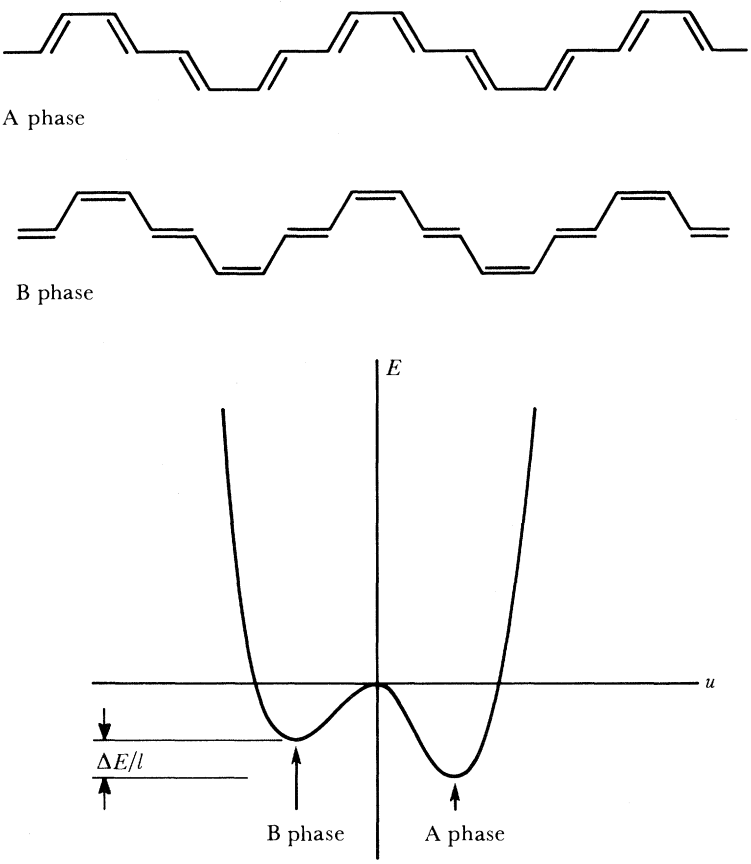

FIGURE 4. Schematic diagram of polythiophene backbone structure, leaving out the sulphur atoms (see figure 2). The two configurations (A phase and B phase) are nearly (but not precisely) degenerate as shown in the diagram at the bottom of the figure, where we plot energy against the distortion parameter, u ($u = 0$) when the bond lengths are equal.

of four carbon all-*trans* segments linked through a *cis*-like unit. In such a structure the ground state is not degenerate (as sketched in figure 4). However, the energy difference per bond, $\Delta E/l$, might be expected to be small; i.e. greater than zero (as in *trans*-$(CH)_x$) but less than that of *cis*-$(CH)_x$. An obvious consequence of the lack of degeneracy is that the schematic PT structure of figure 4 cannot support stable soliton excitations (Brazovskii 1979, 1980; Brazovskii *et al.* 1981; Fesser *et al.* 1983; Heeger 1981*a*; Lauchlan *et al.* 1981; Brédas *et al.* 1981, 1983) because creating a soliton pair separated by a distance d would use an energy of about $d(\Delta E/l)$. This linear 'confinement' energy leads to bipolarons as the lowest energy charge transfer configurations in such a chain, with creation energy somewhat greater than $(4/\pi)\Delta$ (the creation energy for a bipolaron goes to (1) in the limit of zero confinement). The corresponding energy level diagram (for a positive bipolaron) is sketched in figure 3*b*. The two gap states are for a positive bipolaron (charge $2|e|$) and filled for a negative bipolaron (charge $-2|e|$).

III. Solitons in polyacetylene: some experimental results

(*a*) *In situ visible–i.r. absorption studies of trans-*$(CH)_x$

Electrochemical studies (Nigrey *et al.* 1979, 1981 *a*, 1981 *b*; McInnes *et al.* 1981) have allowed, for the first time, precise control of the doping process and quantitative measurement of the dopant concentration. The *in situ* visible–i.r. absorption studies (Feldblum *et al.* 1982) when combined with electrochemical voltage spectroscopy (Kaufman *et al.* 1982) (e.v.s.) demonstrate that the charge is stored in the mid-gap states. Moreover, the e.v.s. data give directly the energies for charge injection and removal (Kaufman *et al.* 1982, 1983). Analysis of these data yields a value for the soliton formation energy, E_S, in good agreement with (1).

The results (Feldblum 1982) of *in situ* measurements (performed during electrochemical doping) of the visible–i.r. absorption in *trans*-$(CH)_x$ are shown in figure 5. As the doping

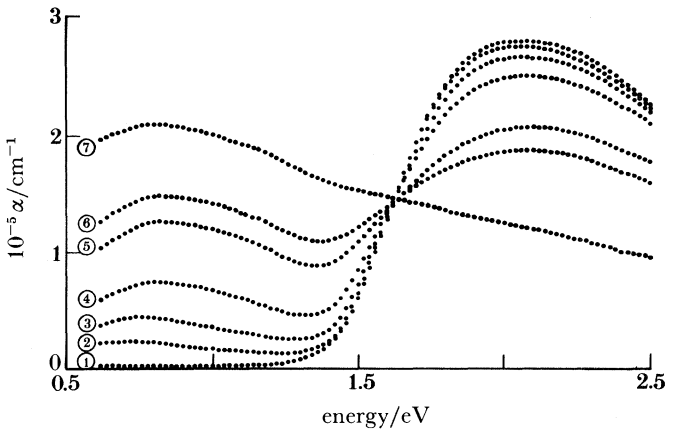

Figure 5. *In situ* absorption curves for *trans*-$(CH)_x$ during electrochemical doping with $(ClO_4)^-$. The applied voltages (against Li) and corresponding dopant concentrations are as follows; curve 1, 2.2 V ($y = 0$); curve 2, 3.28 V ($y = 0.03$); curve 3, 3.37 V ($y = 0.0065$); curve 4, 3.46 V ($y = 0.012$); curve 5, 3.57 V ($y = 0.027$); curve 6, 3.64 V ($y = 0.047$); curve 7, 3.73 V ($y = 0.078$).

proceeds, the mid-gap absorption appears, centred near 0.65–0.75 eV with an intensity that increases monotonically in proportion to the dopant concentration. These spectroscopic features are independent of dopant species and independent of whether the doping is p-type (oxidation) or n-type (reduction) (Kaufman *et al.* 1984). Figure 6 shows optical absorption spectra for polyacetylene doped with different species (Na, Li, Bu_4N, ClO_4) at $y \approx 1\%$. The Na samples were chemically doped and the others electrochemically (using *in situ* opto-e.v.s. technique). The similarity between these data proves conclusively that the optical spectra of *trans*-$(CH)_x$ depends only on the properties of the doped polymer, and not on the particular dopant species.

The mid-gap optical absorption provides direct evidence for charged soliton states in doped polyacetylene. Independent evidence has been obtained from the doping-induced modes (Fincher *et al.* 1979; Etemad *et al.* 1981 *a*) that appear in the mid-infrared associated with the local vibrational modes of the charged bond-alternation domain wall. Again, these mid-infrared modes are independent of dopant (Etemad *et al.* 1982) and show characteristic shifts after deuteration (Etemad *et al.* 1981 *a*), i.e. for $(CD)_x$ compared with $(CH)_x$. That all of these spectroscopic features are associated with charged solitons has been proved unambiguously

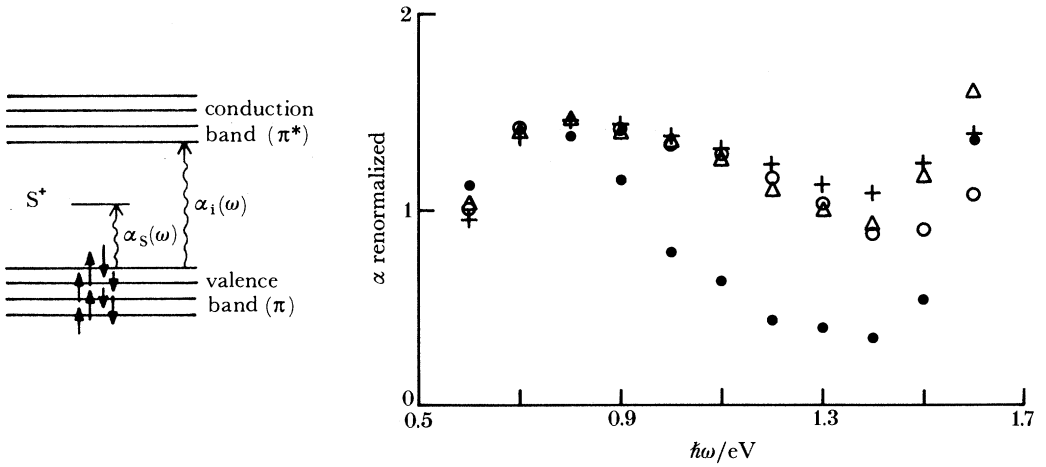

FIGURE 6. Near-i.r. absorption spectra showing the mid-gap transition for *trans*-$(CH)_x$ doped with Na^+, ●; Li^+, △; Bu_4N^+, ○; ClO_4^-, + (Kaufman, 1984).

through a series of photoinduced absorption (Blanchet *et al.* 1983*a*, *b*; Vardney *et al.* 1983) and photoinduced e.s.r. measurements (Flood *et al.* 1981, 1982).

The remarkable oscillator strength associated with these doping-induced spectroscopic features arises directly from the spatial extent of the charge storage state (Suzuki 1980*a*, *b*). Whereas one might anticipate that the ratio of oscillator strengths would be equal to the dopant concentration, a detailed theoretical analysis shows that for dilute concentrations the mid-gap transition is enhanced by a factor of about $2l$ where $2la$ is the full width of the bond-alternation domain wall and a is the carbon–carbon spacing along the $(CH)_x$ chain. Because $2l \approx 14$, this enhancement of the soliton transition makes it observable even at highly dilute dopant concentrations. A complete analysis of the strength of the mid-gap transition is included in the work of Feldblum *et al.* (1982), who find the results to be in good quantitative agreement with theory.

(*b*) *Photoinduced absorption studies of trans*-$(CH)_x$

Information on the intrinsic properties of the nonlinear soliton excitations has been obtained from a series of photoinduced absorption experiments. These studies were simulated by the calculations of Su & Schrieffer (1980*b*), which showed that solitons could be photogenerated. Their results demonstrated that in *trans*-$(CH)_x$ an electron–hole pair should evolve into a pair of solitons within an optical phonon period, or about 10^{-13} s. Photoinduced excitations have been observed and their dynamics have been studied. These experimental results on the photoinduced (p.i.) changes in absorption confirmed the predictions and established the reversed spin–charge relation of the soliton model.

The photogeneration of soliton–antisoliton pairs implies formation of states at mid-gap. Time-resolved spectroscopy (Orenstein *et al.* 1982) has been used to observe the predicted absorption from photogenerated intrinsic gap states. Moreover, the time scale for photogeneration of these gap states has been investigated (Shank *et al.* 1982; Vardeny *et al.* 1982). With the use of sub-picosecond resolution, these studies demonstrated that the gap states and the associated interband bleaching are produced in less than 10^{-13} s, consistent with the theoretical predictions.

Vardeny *et al.* (1983) and Blanchet *et al.* (1983*a*, *b*) have observed the photoinduced absorption arising from both the mid-gap electronic transition (sketched on figure 2) and the associated infrared active modes introduced by the local lattice distortion. The results of Blanchet *et al.* (1983*a*) are reproduced in figure 7. The 0.5 eV absorption arises from the mid-gap transition. The i.r. modes at 1370 and 1260 cm^{-1} are consistent with the calculations of Melé & Rice (1980) and Horowitz 1980) that predict the appearance of i.r. active internal vibrational modes between each of the Raman modes of pure *trans*-$(CH)_x$.

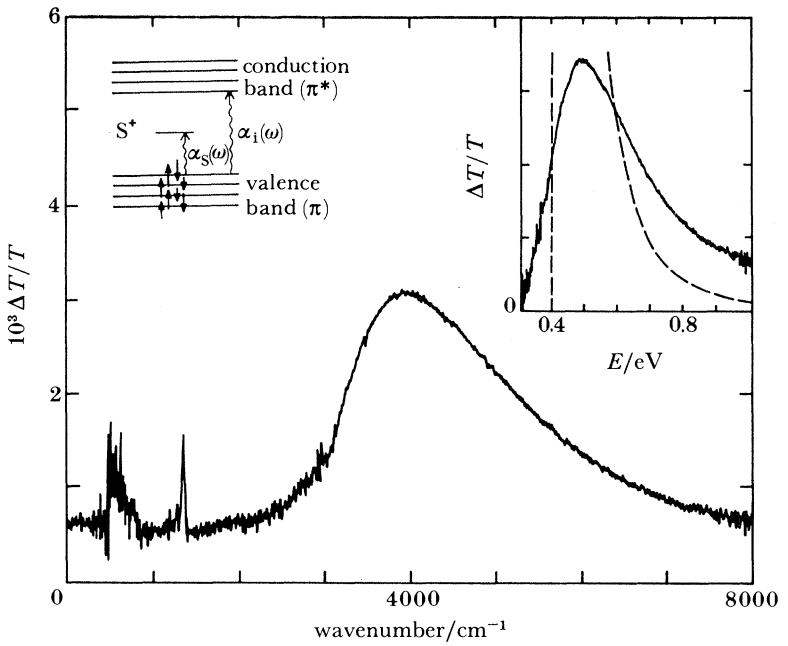

FIGURE 7. Photoinduced absorption in *trans*-$(CH)_x$ (see Blanchet 1983*a*). The solitons are photogenerated by using photons with $\hbar\omega > E_g$. The subsequent photoinduced absorption process (that occurs at *ca.* 0.5 eV) involving the mid-gap state for a positive soliton is shown (left inset). A similar process (mid-gap to conduction band) occurs for the negative soliton. The infrared bands at 1370 and 1260 cm^{-1} provide information on the internal vibrational modes of the photogenerated domain walls. The peak at 500 cm^{-1} is the 'pinned' mode (see text). The mid-gap transition is shown more clearly in the upper right; it has the characteristic asymmetry expected for the theoretical lineshape (broken curve) (Blanchet 1983).

Infrared spectroscopy studies (Fincher *et al.* 1979; Etemad *et al.* 1981*a*, 1982) of lightly doped *trans*-$(CH)_x$ have demonstrated that the same spectroscopic features arise upon doping. Moreover, these doping-induced absorptions are independent of the dopant and are therefore identified as intrinsic features of the doped *trans*-$(CH)_x$ chain. These important results demonstrate that both the photoinduced spectroscopic features and those induced by doping are associated with the same charged state. Moreover, the observed frequencies and lineshapes are consistent with those expected for charged soliton excitations (Etemad *et al.* 1981*a*, 1982). It has been argued (Horowitz 1980) that these changes in infrared absorption are general features of charged localized states on the *trans*-$(CH)_x$ chain (solitons or polarons) and thus not definitive proof of the photogeneration of solitons. However, because these excitations have the reversed spin–charge relation of solitons, this ambiguity is settled (Flood *et al.* 1981, 1982). Thus, for example, the p.i. modes can be used as signatures of soliton formation.

The energy of the p.i. 'mid-gap' transition (*ca.* 0.5 eV, see figure 7) is not precisely $E_g/2$ ($E_g \approx 1.4-1.5$ eV) (Ozaki *et al.* 1979, 1980; Tani *et al.* 1980*a*, *b*; Grant *et al.* 1981; Moses *et al.* 1982*a*). The shift of *ca.* 0.3 eV most probably results from the electron–electron Coulomb interaction. Because the initial state involves two electrons (or holes) in the mid-gap level and the final state involves one electron, the inclusion of the Coulomb interaction into the model (Feldblum *et al.* 1982; Kivelson *et al.* 1982) lowers the energy of the transition by an amount consistent with that expected for the spatially extended soliton wavefunction.

The photogeneration process considered by Su & Schrieffer (1980*b*) is indirect and occurs via an electron–hole excitation as an intermediate step. The incident photon generates an electron–hole pair ($\hbar\omega > 2\Delta$), and the lattice then distorts around the photogenerated charge carriers, leading to a soliton–antisoliton ($S^+\bar{S}^-$) pair. Etemad *et al.* (1981*b*) proposed the direct photogeneration of $S^+\bar{S}^-$ pairs, which would begin at $2E_S = (4/\pi)\Delta$ where E_S is the soliton creation energy. Sethna & Kivelson (1982) and Su & Yu (1983) calculated this direct transition rate. The effects of nonlinear ground-state quantum fluctuations were necessarily included since the direct photogeneration of a soliton pair requires a significant lattice distortion with a simultaneous electronic transition. In this context, the direct photoproduction of $S\bar{S}$ pairs is particularly interesting for it probes the quantum nature of the nonlinear soliton excitations. This direct process requires that ground-state fluctuations (instantons) be present to prepare the system for the photoproduction of a real soliton pair. Consequently the quantum efficiency is predicted to be small near threshold and to increase exponentially (Sethna *et al.* 1982; Su *et al.* 1983) as $\hbar\omega$ approaches 2Δ.

An experimental study of the excitation profile has been carried out by using the p.i. absorption as a direct measure of excitation density (Blanchet *et al.* 1983*b*). Figure 8 shows the excitation profile; i.e. the strength of the photoinduced i.r. absorptions as a function of the photon energy of the pump. The abscissa represents the strength of 1370 cm^{-1} mid-i.r. mode;

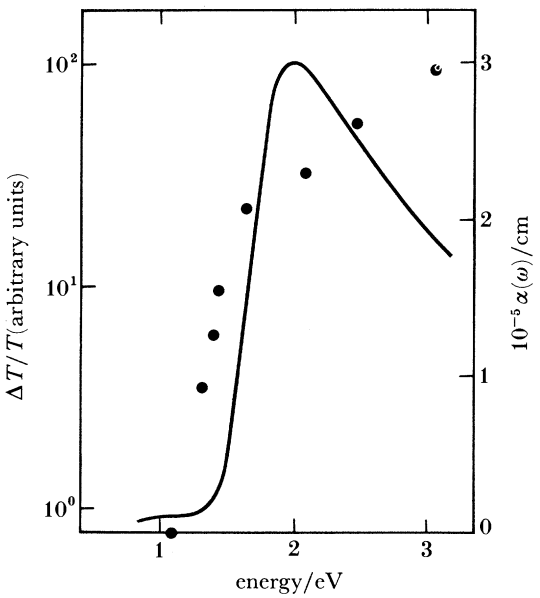

FIGURE 8. Excitation profile (○) for the 1370 cm^{-1} band in *trans*-$(CH)_x$. The intensity of this mode (i.e. the relative excitation density) is plotted against pump frequency. The solid curve is the absorption coefficient against energy (Blanchet 1983*b*).

PHILOSOPHICAL TRANSACTIONS OF THE ROYAL SOCIETY A MATHEMATICAL, PHYSICAL & ENGINEERING SCIENCES

the ordinate is the frequency of the pump that was varied from 1.1 eV (well below the energy gap) to 3.0 eV. The photoexcitation profile in figure 8 shows two distinct regions, both with exponential behaviour. The onset for photoproduction of solitons is slightly above 1.0 eV; the excitation profile increases rapidly for photon energies up to about 1.5 eV and more slowly thereafter. Comparison with the absorption spectra (solid curve, figure 8) indicates that the threshold for the p.i. signal is well below the energy gap.

Figure 8 demonstrates that the onset of photoproduction is below the principal absorption edge, and consequently direct photoproduction of solitons occurs at photon energies less than $E_g \equiv 2\Delta$. While the interpretation (Etemad *et al.* 1981*b*) of the subgap photoconductivity was speculative, the i.r. signatures in the data presented by Blanchet *et al.* (1983*b*) are specific; they provide an unambiguous measurement of the excitation density and demonstrate direct photoproduction of solitons. The predicted threshold for direct photoproduction is (from (1)) $2E_S = (4/\pi)\Delta$. With $E_g \equiv 2\Delta \approx 1.5$–$1.6$ eV, the expected value is $2E_S \approx 1$ eV, in good agreement with figure 8.

The results shown in figure 8 were not corrected for absorption, etc., in the polymer film. In the thin sample limit ($\alpha d < 1$) one expects the number of photogenerated solitons (N_S) to be proportional to the number of absorbed photons,

$$N_S = (1-R)\,(N_0\tau)\,(\alpha d)\,\epsilon, \tag{2}$$

where N_0 is the incident photon flux, α is the absorption coefficient, d is the sample thickness, τ is the excitation lifetime, ϵ is the quantum efficiency and R is the (slowly varying with frequency) reflectivity. The exponential increase in N_S shown in figure 8 implies the existence of an exponential tail (Urbach tail) in the absorption coefficient at energies below the gap. This Urbach tail has recently been measured by Weinberger *et al.* (1984) utilizing a novel direct absorption technique. Their results indicate an exponential increase in $\alpha(\omega)$; $\alpha = \alpha_0 \exp(\omega/\omega_0)$ where the value for ω_0 is in agreement with that inferred from figure 8. Thus the photogenerated solitons originate from photons absorbed in the Urbach tail.

An alternative mechanism for the Urbach tail (and the associated photogeneration of charged solitons) is disorder-induced absorption from localized states below the band edge (Weinberger *et al.*). Such effects might well be expected for polyacetylene in view of the partial crystallinity and fibrillar morphology (Heeger *et al.* 1980, 1981*b*,*c*; Etemad *et al.* 1982). Computer simulations (A. R. Bishop, personal communication) have in fact recently shown that such disorder-induced absorption from defect states in the energy gap can lead to photoproduction of charged solitons. Therefore, the results shown in figure 8 for $\hbar\omega < 1.4$ eV may arise from a combination of two mechanisms; (i) direct photoproduction of $S\bar{S}$ assisted by quantum fluctuations and (ii) photoproduction of $S\bar{S}$ pairs via disorder-induced absorption into localized states.

IV. Bipolarons in polythiophene: *in situ* absorption studies

(*a*) *Experimental results*

Figure 9 shows a series of absorption spectra (Chung *et al.* 1984) taken *in situ* during the doping cycle at different applied voltages: 3.6 V ($y = 2.8\%$), 3.65 V ($y = 4\%$), 3.7 V ($y = 5.4\%$), 3.8 V ($y = 9.6\%$), 3.85 V ($y = 12\%$), 3.9 V ($y = 14\%$), 4.05 V ($y = 20\%$). In each case the cell was allowed to come to quasi-equilibrium before taking the spectra. Doping levels were

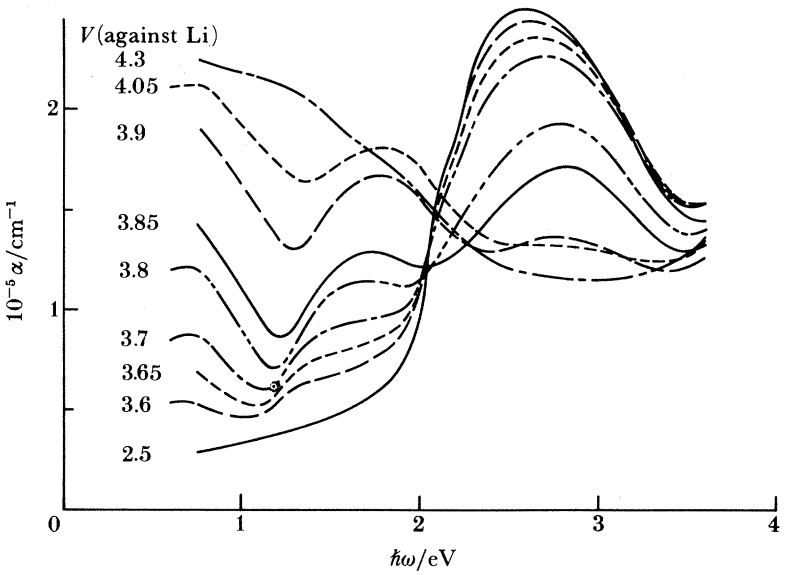

FIGURE 9. *In situ* absorption curves for polythiophene during electrochemical doping with $(ClO_4)^-$. The applied voltages (against Li) are shown on the left. The corresponding concentrations were obtained as e.v.s. measurements and are as follows (in mol % per thiophene ring); 3.60 V ($y = 2.8\,\%$); 3.65 V ($y = 4\,\%$); 3.70 V ($y = 5.4\,\%$); 3.80 V ($y = 9.6\,\%$); 3.85 V ($y = 12\,\%$); 3.90 V ($y = 14\,\%$); 4.05 V ($y = 20\,\%$) (Chung *et al.* 1984).

obtained from direct electrochemical measurements for V_{app} against Q in a parallel experiment using electrochemical voltage spectroscopy (Chung *et al.* 1984).

As the doping proceeded via the oxidation reaction,

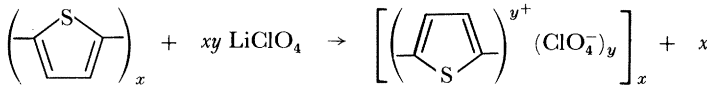

(3)

the intensity of the interband transition decreased continuously and the absorption peak shifted toward higher energy. In addition, the two new absorption features appeared in the i.r. below the gap edge with intensities that increased as the dopant level increased. The lower energy i.r. peak remains at a constant energy (*ca.* 0.65 eV) while the higher energy peak shifts toward higher energy as the dopant level is increased. At 4.3 V, the frequency-dependent absorption is characteristic of the free carrier spectrum of the metallic state, similar to that found in heavily doped (either chemically or electrochemically) polyacetylene (Etemad *et al.* 1982).

The spectra of figure 9 for $\hbar\omega > 0.8$ eV were obtained (Chung *et al.* 1984) by using an identical cell (but with no sample) as reference. However, below 0.8 eV the strong absorption of the electrolyte solution limited the accuracy of the data. The extension of the curves on figure 9 below 0.8 eV was performed on selected individual samples which were doped (to a particular applied voltage) and sealed in a tube without solution.

Better accuracy was obtained by analyzing the difference spectra from the sample (Chung *et al.*). Two examples are shown in figure 10*a* ($V_{app} = 3.65$ V, $y = 1\,\%$ per carbon) and figure 10*b* (3.85 V, $y = 3\,\%$ per carbon). In each case the spectrum was taken at the appropriate applied cell voltage (against Li), and the neutral point spectrum (2.5 V, $y = 0$) was used as the reference. The two dopant-induced infrared bands are seen clearly with peaks at

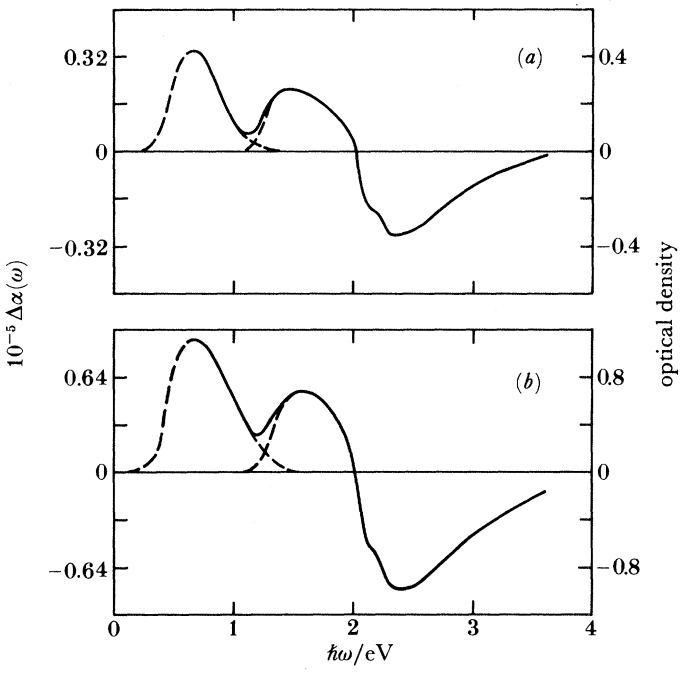

FIGURE 10. Difference spectra obtained from the data of figure 9; (*a*) $V_{app} = 3.65$ V, $y = 4\%$ (or 1% per carbon); (*b*) $V_{app} = 3.85$ V, $y = 12\%$ (or 3% per carbon). In each case the neutral point spectrum ($V_{app} = 2.50$ V) was used as the reference. The broken curves are extrapolations that attempt to separate the contributions from the two absorption peaks (see text; also Chung *et al.* 1984).

$\hbar\omega_1 = 0.65$ eV and $\hbar\omega_2 = 1.5$ eV. As noted above, $\hbar\omega_1$ is essentially independent of dopant concentration whereas $\hbar\omega_2$ increases with increasing frequency. Examination of figures 9 and 10 indicates that the oscillator strength of these two dopant-induced i.r. absorption bands is comparable to that of the mid-gap absorption in polyacetylene (Feldblum *et al.* 1982; Suzuki *et al.* 1980*a*, 1980*b*). We conclude, therefore, that these two absorption features arise from electronic transitions between the valence band and two localized energy levels that appear in the gap upon charge-transfer doping.

The difference spectra of figure 10 show that the oscillator strength that appears below the gap edge comes primarily from the interband transition. In contrast to *trans*-polyacetylene (Feldblum *et al.* 1982; Suzuki *et al.* 1980*a*, *b*) the loss of interband oscillator strength is not uniform but is greatest for frequencies near the band edge.

A procedure similar to that described above was performed (Chung *et al.* 1984) in the subsequent electrochemical undoping process by using a series of stepped-down constant applied potentials. The electrochemical reaction is the reverse of (3). At $V_{app} = 2.5$ V, the spectrum of undoped polythiophene was reproduced (Chung *et al.*).

Both on the doping and on the undoping parts of the cycle, an isosbestic point appears at $\hbar\omega = 2.0$ eV for dilute doping levels. At higher dopant concentrations (e.g. for $V_{app} > 3.85$ V, $y < 3\%$ per carbon) this isosbestic point disappears and the spectrum qualitatively changes, evolving toward that of the metallic limit.

(*b*) *Discussion in terms of confined* $S\bar{S}$ *pairs or bipolarons*

The absorption spectrum of neutral polythiophene is remarkably similar to that of *trans*-$(CH)_x$ (Feldblum *et al.* 1982; Suzuki *et al.* 1980) but blue-shifted by about 0.4–0.5 eV. Even the familiar structure on the leading edge, attributed by Melé (1982, 1984) to dynamical chain distortion following electron–hole creation, is evident in the data. These similarities suggest that polythiophene can be viewed as similar to *trans*-$(CH)_x$, but with the ground-state degeneracy lifted by a small amount because of the inequivalence of the two structures with opposite bond alternation. This analogy was emphasized in the schematic structure shown in figure 2.

Although this description of PT is admittedly schematic, there is experimental evidence that it represents an excellent starting point for a more detailed description of the doping processes in this system. The optical absorption data (figures 9 and 10) indicate an energy level structure at dilute doping levels as shown in figure 3*b* with $\hbar\omega_1$ and $\hbar\omega_2$ just below the peaks because the transitions involved are between a localized gap state and the valence band density of states. The value for the interband absorption can be estimated from the data of figures 9 and 10 to be $\hbar\omega_I \approx 2.1$ eV. In this case, the joint density of states of the valence and conduction bands is involved in the absorption so that the point of steepest slope in $\alpha(\omega)$ or the crossover in the difference curves (figure 10) is used. Although there is surely some uncertainty in the assignment of the precise energies, the data from the dilute dopant concentrations yield

$$\hbar\omega_1 + \hbar\omega_2 \approx \hbar\omega_I = E_g, \tag{4}$$

where $E_g \equiv 2\Delta_0$ is the energy gap. The results expressed quantitatively in (4) indicate the existence of electron–hole symmetry in the doped polymer. Referring to figure 3*b*, the two doping-induced energy levels appear symmetrically with respect to the gap centre at $\pm\hbar\omega_0 = 0.40 \pm 0.05$ eV. The existence of electron–hole symmetry implies that the schematic structure of figure 4 represents an essentially correct point of view. The sulphur atoms stabilize the polyene chain in the configuration of figure 4 through covalent bonding to neighbouring carbon atoms. However, evidently the sulphur is only weakly interacting with the π-electron system of the polyene backbone. If this were not the case, some of the transferred charge would reside on the sulphur, and the electron–hole symmetry implied by figures 9 and 10 and sketched in figure 3*b* would not be present.

We assign the two energy gap states inferred from figures 9 and 10 to the two levels expected from charge storage in bipolaron states in doped PT (Brazovskii 1979, 1980; Brazovskii *et al.* 1981; Fesser *et al.* 1983; Heeger 1981*a*; Lauchlan *et al.* 1981; Brédas *et al.* 1981, 1983). This assignment is based on three facts.

(i) The two transitions imply formation of two levels symmetric with respect to the gap centre.

(ii) The observation of only two transitions implies that the two levels are not occupied. If there were electrons in the lower level (as there would be for a 'hole' polaron) then a third absorption would be evident, arising as a transition between the two localized levels. This is not observed.

(iii) Analysis of the data leads to $(\omega_0/\Delta_0) \approx 0.35$. This small value is inconsistent with polaron formation for which $(\omega_0/\Delta_0) \geqslant 0.707$ (Brazovskii 1979, 1980; Brazovskii *et al.* 1981; Fesser *et al.* 1983).

The small value inferred for (ω_0/Δ_0) implies weak confinement. By using the results of Fesser

et al. (1983) in their detailed analysis of the bipolaron problem, we can extract values for the relevant microscopic parameters. The confinement parameter is defined as

$$\gamma = \Delta_e/\lambda\Delta_0, \tag{5}$$

where Δ_e is the constant external gap parameter ($2\Delta_e$ would be the energy gap without the bond alternation contribution, Δ_i, which arises from the spontaneous symmetry breaking arising from the Peierls instability), λ is the dimensionless electron–phonon coupling constant appropriate to the twofold commensurate case, and Δ_0 is the full gap parameter ($\Delta_0 = \Delta_e + \Delta_i$). From figure 4 of Fesser *et al.* (1983) we obtain $\gamma \approx 0.1$–0.2 using the experimental value $(\omega_0/\Delta_0) \approx 0.35$. This small value for γ, implying weak confinement, is consistent with the point of view expressed in figure 4 and with the remarkable similarity of the shape of the absorption curves of neutral *trans*-$(CH)_x$ and neutral PT.

The one-dimensional energy gap in *trans*-$(CH)_x$ has been estimated as $E_g^{1D} \approx 1.6$–1.8 eV (Moses 1982*a*). Taking the value of $E_g^{1D} \approx 2.1$ eV for polythiophene, we estimate $\Delta_e \approx 0.15$–0.2 eV. Thus, for (5), we find $\lambda \approx 0.5$–1 for PT. Although this is quite clearly not a precise determination of λ, the resulting value is reasonable. Note that even though the sulphur appears to play only a minor role in the π-electron structure of PT, the bonding to neighbouring carbons to form the heterocycle may lead to significant contributions to the chain stiffness, phonon dispersion, and to the electron-coupling constant, etc.

The relative intensities of the two gap absorptions, $\hbar\omega_1$ and $\hbar\omega_2$, can be obtained from figure 10. Although *in situ* configuration does not allow data acquisition at frequencies below about 0.6 eV, the overall features are clear (we have sketched the extrapolated shape of $\hbar\omega$ to lower frequencies based on the lineshape expected for a transition between a localized state and a one-dimensional band). The lower energy peak has the greater integrated intensity by a factor of about 2; i.e. $I(\omega_1)/I(\omega_2) \approx 2$. This ratio has been calculated by (Fesser *et al.* 1983). They find $I(\omega_1) > I(\omega_2)$ for bipolarons, in agreement with the experimental results; but with $(\omega_0/\Delta_0) \approx 0.35$ they predict $I(\omega_1)/I(\omega_2) \approx 6$. The origin of this discrepancy is not clear. However, it is obvious that the model is oversimplified in many ways. Particularly, in calculating intensities of transitions where the details of the wavefunctions are important, such a quantitative discrepancy is not surprising.

In the case where the ground state is degenerate, the mid-gap transitions steal oscillator strength uniformly from the interband transition. This has been observed and experimentally verified in the *in situ* opto-electrochemical spectroscopy studies of *trans*-$(CH)_x$ (Feldblum *et al.* 1982). For PT, this is not the case. Figures 9 and 10 demonstrate that as the doping proceeds, the interband transition weakens, but not uniformly. The loss of oscillator strength is greater near the interband edge causing the apparent shift to higher energies with increasing dopant concentration. Although a detailed quantitative comparison is difficult, Fesser *et al.* (1983) have shown (see figure 9 of their paper) that the loss of oscillator strength, $\beta(\omega)$, is greater near the band edge in the case of bipolarons. By using $(\omega_0/\Delta_0) \approx 0.35$ (appropriate to PT), $\beta(\omega)$ is two times greater for $\hbar\omega \approx E_g$ than the corresponding value at higher energies. Thus the qualitative features of the observed changes in interband absorption are in excellent agreement with the predictions based on charge storage in bipolarons. A more detailed analysis is not possible at present because of the limited spectral range currently available.

As the dopant concentration is increased $\hbar\omega_1$ remains essentially constant, whereas $\hbar\omega_2$ shifts

toward higher energies. This concentration-dependent shift is not expected within the confines of the non-interacting bipolaron theory. The shift may signal the importance of interactions between bipolarons leading at sufficiently high concentrations to the metallic state. Alternatively the shift may imply some involvement of the sulphur heteroatom at high dopant levels leading to a breakdown of the precise electron–hole symmetry. We note in this context that the electron spin resonance line of heavily doped metallic PT (doped with AsF_5) exhibits a small g-shift (2.008) relative to that of polyacetylene under similar conditions (2.0026), implying some charge on the sulphur heteroatom at high dopant levels (Moraes *et al.* 1985).

In the heavily doped limit ($V_{app} = 4.3$ V), all signs of the interband transition have disappeared, and the spectrum (figure 9) is dominated by the free carrier absorption in the infrared. In this régime, the optical properties of doped PT are those of a metal. The magnitude and spectral dependence of $\alpha(\omega)$ are similar to those reported earlier (Chung *et al.* 1981, 1983) for Na-doped *trans*-$(CH)_x$ where electrical conductivities in excess of $10^3\ \Omega^{-1}$ cm were inferred from the frequency-dependent absorption in the i.r. and subsequently observed directly in d.c. measurements (Chung *et al.* 1983). Thus, metallic doped PT can be expected to be an excellent conductor. Although previous conductivity measurements on electrochemically synthesized (and doped) PT have yielded values (Kaneto *et al.* 1983) as high as $100\ \Omega^{-1}$ cm, the intrinsic values may in fact be much higher.

(*c*) *Electrochemical voltage spectroscopy of polythiophene*

The e.v.s. measurements (figure 11) provide complementary information. Charge injection (oxidation) occurs above about 3.45 ± 0.05 V against Li. Because the neutral point is at 2.5 V (against Li) this charge injection threshold implies $\Delta_0 \approx 0.95 \pm 0.05$ eV. Preliminary attempts at n-doping (reducing) the polymer exhibited a threshold at about 1.6 eV, indicating approximate symmetry about the neutral point and an electrochemically determined energy gap of about 1.9 eV. A value slightly smaller than the optical gap is expected because initial injection should occur as a single polaron at an energy of about $0.9\Delta_i$ (in the weak confinement limit, approaching Δ_0 as γ increases).

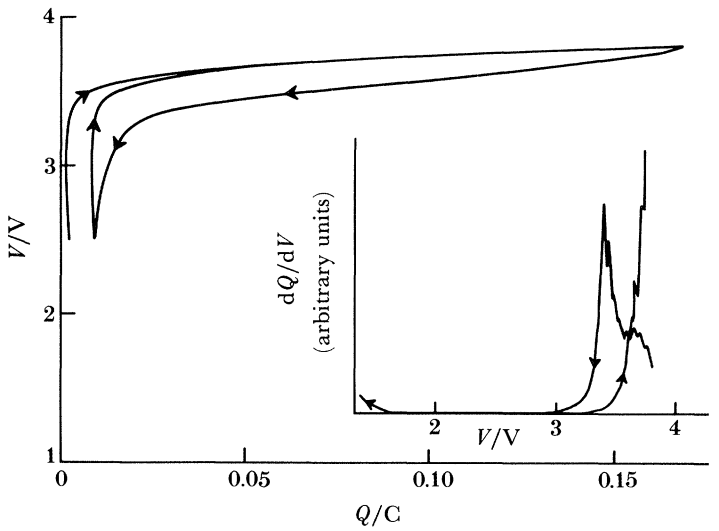

FIGURE 11. V against Q (in coulombs) for polythiophene against Li; the inset shows dQ/dV against V for the same cycle (Chung *et al.* 1984).

Hysteresis is observed in the V against Q cycle, reminiscent of similar effects reported earlier for polyacetylene (Kaufman *et al.* 1983, 1984). A detailed analysis (Kaufman *et al.* 1983, 1984) of the many contributions to the free energy has been carried out for polyacetylene leading to the conclusion that the hysteresis is intrinsic; charge is injected near the band edge, but stored in gap centre states associated with soliton pairs generated by structural relaxation around the injected charges. In polythiophene, because the ground state is non-degenerate, the corresponding coupling of the π-electron to chain distortions leads to a splitting of the mid-gap states into the symmetric bipolaron levels and to charge storage in the bipolaron gap states, as demonstrated by the analysis of the visible–i.r. absorption data. Thus, in PT, the hysteresis in V against Q arises from charge injection near the band edge (single polarons), and charge removal from the bipolaron gap states. Note that because bipolarons can exist only in the doubly charged state, removal of a charge will yield a charged polaron. The identification of the maximum in $\mathrm{d}Q/\mathrm{d}V$ (on removal) with the bipolaron chemical potential therefore relies on the infrared absorption data that show no evidence of single polarons either on the doping or the undoping parts of a cycle. Evidently the kinetics of the recombination of polaron pairs into lower energy bipolarons is sufficiently rapid in polythiophene that no significant polaron population is ever achieved. For polypyrrole, where the kinetics are slower, the optical data and the chemical potential for charge removal appear to result from a combination of polarons and bipolarons in the sample (Scott *et al.* 1984; Kaufman *et al.* 1984).

The magnitude of the hysteresis ΔV quantitatively locates the chemical potential of the doped polymer (at dilute doping levels),

$$\mu = \Delta_0 - \Delta V$$

measured with respect to the centre of the energy gap. By using $\Delta_0 \approx 1.05$ eV and $\Delta V \approx 0.3$ eV (see figure 9) we find $\mu \approx 0.7\,\Delta_0$. This value is slightly larger than that expected ($\mu = 2\Delta/\pi$) for the degenerate ground-state limit where the confinement parameter is zero (Kaufman *et al.* 1984). The experimental value is therefore consistent with the weak confinement inferred from analysis of the *in situ* spectroscopy data.

Battery cells have been constructed with PT films grown from dithiophene on platinum foil (Chung *et al.* 1984; Kaufman *et al.* 1984). Throughout the dopant range from 0–20% per thiophene ring (*ca.* 4.0% per carbon) we obtained Coulomb efficiences greater than 95%. Cycles to cell potentials greater than 4.0 V yielded better than 85% efficiency at doping levels greater than 5.0% per carbon. Thus, without resorting to extraordinary techniques to ensure purity, we have found excellent electrochemical stability. After charging such a cell to an open circuit voltage of 3.8 V, corresponding to *ca.* 4.5% doping (per carbon), short circuit currents of about 20 mA/mg were obtained. At the same concentration, the maximum power density was 2.5×10^4 W kg^{-1}, based on the weight of doped polymer and the mass of lithium consumed. E.v.s. cycles up to 4.2 V (*ca.* 6% per carbon) demonstrated an energy density of 140 W hr kg^{-1} normalized in the same way. Corresponding values for polyacetylene (against Li) cells at 6% (per carbon) doping are *ca.* 25 mA mg^{-1} (short circuit current), *ca.* 3×10^4 W kg^{-1} (maximum power density), and *ca.* 176 W h kg^{-1} (energy density). The latter numbers are also based on the weight of the doped polymer and the mass of lithium consumed. These numbers are for comparison only; corresponding values for packaged cells would be lower.

PHILOSOPHICAL TRANSACTIONS OF THE ROYAL SOCIETY A MATHEMATICAL, PHYSICAL & ENGINEERING SCIENCES

V. Solitons in *trans*-$(CH)_x$: collective transport by mobile, spinless, charged solitons?

The experimental studies summarized above demonstrate that in doped polyacetylene, charge is stored in the mid-gap states of the doping-induced charged solitons. Are these charged solitons also involved in the electrical transport? The answer appears to be that they are; either they are mobile and take part directly in the transport, or they are pinned with electrons moving through the mid-gap band of levels through variable range hopping.

Because of the complications that arise from the possibility of non-uniform doping, and from uncertainty in the precise nature of the dopant species (e.g. AsF_4^- or AsF_6^-, or both, the demonstration of spinless charge carriers, the mechanism of the semiconductor–metal transition and the nature of the transitional régime in *trans*-$(CH)_x$ have been controversial. Ikehata *et al.* (1980) were the first to present data indicating that the magnetic susceptibility (χ) was insensitive to dopant concentration and remained smaller than that of the metallic state throughout the transitional régime (*ca.* 1–5 mol %). On the other hand, Tomkiewicz *et al.* (1979, 1981) presented data that showed a continuous increase in the Pauli susceptibility (χ_P) and argued that this behaviour resulted from the continuous formation of metallic islands, with the final transition to the metallic state being coincident with the percolation threshold.

In an attempt to resolve these important experimental issues, an experimental study of $[Na_y^+(CH)^{y-}]_x$ was recently completed (Chung *et al.* 1983) in the concentration range $y < 0.1$. Through coordinated measurements of the magnetic susceptibility, optical properties, and d.c. conductivity on the same samples in a sealed apparatus, it was demonstrated that χ_P remains small (less than 10^{-8} e.m.u. mol^{-1}†) for $y < 0.05$, rising abruptly for $0.05 < y < 0.06$ by more than two orders of magnitude to $\chi_P \approx 2 \times 10^{-6}$ e.m.u. mol^{-1}, typical of the metallic state. The principal results (Chung *et al.* 1983) are summarized in figure 12 where we plot χ_P (right hand scale) and $\sigma_{d.c.}$ (300K) (left hand logarithmic scale) for direct comparison. Throughout the régime $y < 0.05$, we infer $\chi_P < 10^{-8}$ e.m.u. mol^{-1}. The quality of the samples and procedures can be further evaluated by noting that in the heavily doped metallic régime, σ is in excess of $10^3\ \Omega^{-1}$ cm^{-1}, more than an order of magnitude greater than previously reported.

Two mechanisms have been proposed to explain the relatively high conductivity in the régime $0.001 < y < 0.05$, where $\chi_P \approx 0$; both involve charged solitons in the transport process. The simultaneous existence of high electrical conductivity in the régime led to the suggestion (Ikehata *et al.* 1980; Moses *et al.* 1982*b*) that the conduction in the régime is due to unpinned charged solitons and that the final transition to truly metallic behaviour occurred abruptly at dopant levels above 5 mol %. The persistence of the mid-gap transition and the soliton-induced infrared modes throughout the régime (Rabolt *et al.* 1979) provided support for this interpretation. Alternatively, Epstein *et al.* (1983) followed the suggestion of Melé & Rice (1981) and attempted to explain the moderately high conductivity in terms of the variable range hopping (v.r.h.) model (Mott *et al.* 1979). In this case, the charged solitons are considered to be pinned with the associated 'mid-gap' electronic states distributed into a band. Because of disorder in the polymer, it is proposed by Epstein *et al.* (1983) that there is a finite density of such states at E_F, thereby allowing variable range hopping.

Dong & Schrieffer (1985) have demonstrated that an 'insulator–metal' transition from

† $\chi_{c.g.s.} = M/H$; $\chi_{SI} = \mu_0 M/H$.

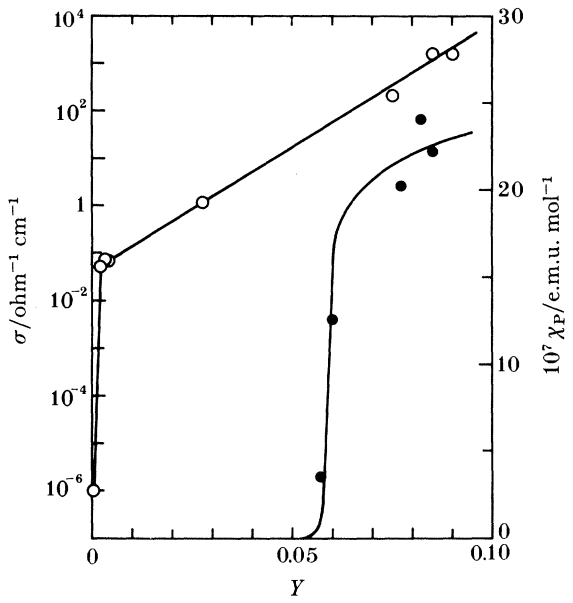

FIGURE 12. Room temperature electrical conductivity, σ, and temperature-independent Pauli susceptibility, χ_P against dopant concentration for $[Na_y^+(CH)^{y-}]_x$ (Chung *et al.* 1983).

pinned to mobile solitons is to be expected at concentrations in this régime. However, it is unlikely that the transport mechanism can be determined from traditional transport measurements alone. Both mobile solitons and v.r.h. through soliton levels involve hopping of charge with associated non-activated behaviour, frequency dependence, etc. To determine whether or not mobile charged solitons contribute to this a specific unambiguous experiment is required. Dong & Schrieffer note that if the solitons are mobile, any band alternation will be motionally narrowed. On the contrary, electron hopping among pinned soliton states will leave the bond alternation constant in time (with a distribution of values as a result of the high concentration of solitons). Thus, a structural analysis of the bond alternation in the relevant concentration range should be capable of resolving this important issue.

VI. CONCLUSION

Extensive studies of polyacetylene have demonstrated that the coupling of electronic excitations to nonlinear conformational changes is an intrinsic and important feature of conducting polymers. Although this coupling and the degenerate ground state together lead to the novel soliton excitations in *trans*-$(CH)_x$, generalization of these concepts and application to the larger class of conjugated polymers has been an obvious goal of the field. The experimental evidence of electron–hole symmetry and weak confinement in polythiophene makes this polymer a nearly ideal example of a model system in which the ground-state degeneracy has been lifted. The study of bipolarons (or confined charged solitons) in polythiophene has demonstrated that the concepts carry over in detail and that a quantitative understanding of the resulting phenomena is possible even for relatively complex systems.

References

Blanchet, G. B., Fincher, C. R., Chung, T.-C. & Heeger, A. J. 1983 *Phys. Rev. Lett.* **50**, 1938.
Blanchet, G. B., Fincher, C. R. & Heeger, A. J. 1983 *Phys. Rev. Lett.* **51**, 2132.
Brazovskii, S. A. 1979 *JETP Lett.* **28**, 656.
Brazovskii, S. A. 1980 *JETP Lett.* **78**, 677.
Brazovskii, S. A. & Kirova, N. 1981 *JETP Lett.* **33**, 4.
Brédas, J. L., Chance, R. R. & Silbey, R. 1981 *Molec. Cryst. Liq. Cryst.* **77**, 319.
Brédas, J. L., Themans, B., Andre, J. M., Chance, R. R., Boudreaux, D. S. & Silbey, R. 1983 *J. Phys., Paris* **44**, 373.
Chung, T.-C., Feldblum, A., Heeger, A. J. & MacDiarmid, A. G. 1981 *J. chem. Phys.* **47**, 5504.
Chung, T.-C., Kaufman, J. H., Heeger, A. J. & Wudl, F. 1984 *Phys. Rev.* B **30**, 702.
Chung, T.-C., Moraes, F., Flood, J. D. & Heeger, A. J. 1983 *Phys. Rev.* B **29**, 2341.
Dong, J. & Schrieffer, J. R. 1985 (In preparation.)
Epstein, A. J., Rommelman, H., Bigelow, R., Gibson, H. W., Hoffman, D. M. & Tanner, D. B. 1983 *Phys. Rev. Lett.* **50**, 1866.
Etemad, S., Pron, A., Heeger, A. J., MacDiarmid, A. G., Mele, E. J. & Rice, M. J. 1981*a* *Phys. Rev.* B **23**, 5137.
Etemad, S., Mitani, M., Ozaki, M., Chung, T.-C., Heeger, A. J. & MacDiarmid, A. G. 1981*b* *Solid St. Commun.* **40**, 75.
Etemad, S., Heeger, A. J. & MacDiarmid, A. G. 1982 *A. Rev. Phys. chem.* **33**, 443–469.
Feldblum, A., Kaufman, J. H., Etemad, S., Heeger, A. J., Chung, T.-C. & MacDiarmid, A. G. 1982 *Phys. Rev.* B **26**, 815.
Fesser, K., Bishop, A. R. & Campbell, D. K. 1983 *Phys. Rev.* B **27**, 4804.
Fincher, C. R., Ozaki, M., Heeger, A. J. & MacDiarmid, A. G. 1979 *Phys. Rev.* B **19**, 4140.
Flood, J. D. & Heeger, A. J. 1981 *Phys. Rev.* B **28**, 2356.
Flood, J. D., Ehrenfreund, E., Heeger, A. J. & MacDiarmid, A. G. 1982 *Solid St. Commun.* **44**, 1055.
Grant, P. M., Tani, T., Gill, W. D., Krounbi, M. & Clarke, T. C. 1981 *J. appl. Phys.* **52**, 869.
Heeger, A. J. & MacDiarmid, A. G. 1980 *The physics and chemistry of low-dimensional solids* (ed. L. Alcacer), pp. 353, 393. Dordrecht: Riedel.
Heeger, A. J. 1981*a* *Comments on Solid State Physics* **10**, 53.
Heeger, A. J. & MacDiarmid, A. G. 1981*b* *Chem. Scripta* **17**, 115.
Heeger, A. J. & MacDiarmid, A. G. 1981*c* *Molec. Cryst. Liq. Cryst.* **77**, 1.
Horowitz, B. 1980 *Solid St. Commun.* **41**, 729.
Ikehata, S., Kaufer, J., Woerner, T., Pron, A., Druy, M. A., Sivak, A., Heeger, A. J. & MacDiarmid, A. G. 1980 *Phys. Rev. Lett.* **45**, 1123.
Jackiw, R. & Rabbe, C. 1978 *Phys. Rev.* D **13**, 3398.
Jackiw, R. & Schrieffer, J. R. 1981 *Nucl. Phys.* B **190**, 253.
Kaneto, K., Kohno, Y., Yoshino, K. & Inuishi, Y. 1983 *J. chem. Soc. chem. Commun.*, p. 382.
Kaufman, J. H., Kaufer, J. W., Heeger, A. J., Kaner, R. & MacDiarmid, A. G. 1982 *Phys. Rev.* B **26**, 4.
Kaufman, J. H., Chung, T.-C. & Heeger, A. J. 1983 *Solid St. Commun.* **47**, 585.
Kaufman, J. H., Chung, T.-C. & Heeger, A. J. 1985 *J. electrochem. Soc.* (In the press.)
Kaufman, J. H., Colaneri, N., Scott, J. C. & Street, G. B. 1984 *Phys. Rev. Lett.* **53**, 1005.
Kaufman, J. H., Chung, T.-C., Heeger, A. J. & Wudl, F. 1984 *J. electrochem. Soc.* **131**, 2092.
Kivelson, S. & Heim, D. E. 1982 *Phys. Rev.* B **26**, 4278.
Lauchlan, L., Etemad, S., Chung, T.-C., Heeger, A. J. & MacDiarmid, A. G. 1981 *Phys. Rev.* B **24**, 3701.
McInnes, D., Druy, M. A., Nigrey, P. J., Nairns, D. P., MacDiarmid, A. G. & Heeger, A. J. 1981 *J. chem. Soc. chem. Commun.*, p. 317.
Melé, E. J. & Rice, M. J. 1980 *Phys. Rev. Lett.* **45**, 926.
Melé, E. J. 1984 *J. synth. Metals* **9**, 207.
Melé, E. J. & Rice, M. J. 1981 *Phys. Rev.* B **23**, 5397.
Melé, E. J. 1982 *Solid St. Commun.* **44**, 827.
Moraes, F., Davidov, D., Kobayashi, M., Chung, T.-C., Chen, J., Heeger, A. J. & Wudl, F. 1985 *J. synth. Metals* (In the press.)
Moses, D., Feldblum, A., Denenstein, A., Ehrenfreund, E., Chung, T.-C., Heeger, A. J. & MacDiarmid, A. G. 1982*a* *Phys. Rev.* B **26**, 3361.
Moses, D., Denenstein, A., Chen, J., McAndrew, P., Woerner, T., Heeger, A. J., MacDiarmid, A. G. & Park, Y. W. 1982*b* *Phys. Rev.* B **25**, 7652.
Mott, N. F. & Davis, E. A. 1979 *Electronic processes in non-crystalline materials*. Oxford: Clarendon Press.
Nechtschein, M., Devreaux, F., Green, R. L., Clark, T. C. & Street, G. B. 1980 *Phys. Rev. Lett.* **44**, 356.
Nigrey, P. J., MacDiarmid, A. G. & Heeger, A. J. 1979 *J. chem. Soc. chem. Commun.*, p. 594.
Nigrey, P. J., McInnes, D., Nairns, D. P., MacDiarmid, A. G. & Heeger, A. J. 1981*a* *J. electrochem. Soc.* **128**, 1651.
Nigrey, P. J., MacDiarmid, A. G. & Heeger, A. J. 1981*b* *Molec. Cryst. Liq. Cryst.* **77**.
Orenstein, J. & Baker, G. L. 1982 *Phys. Rev. Lett.* **49**, 1043.

PHILOSOPHICAL TRANSACTIONS OF THE ROYAL SOCIETY A MATHEMATICAL, PHYSICAL & ENGINEERING SCIENCES

Ozaki, M., Peebles, D., Weinberger, B. R., Chiang, C. K., Gau, S. C., Heeger, A. J. & MacDiarmid, A. G. 1979 *Appl. Phys. Lett.* **35**, 83.
Ozaki, M., Peebles, D., Weinberger, B. R., Heeger, A. J. & MacDiarmid, A. G. 1980 *J. appl. Phys.* **51**, 4252.
Rabolt, J. F., Clarke, T. C. & Street, G. B. 1979 *J. chem. Phys.* **71**, 4614.
Rice, M. J. 1979 *Phys. Lett.* A **71**, 152.
Scott, J. C., Bredas, J. L., Yakushi, K. & Street, G. B. 1984 *Phys. Rev.* B **30**, 1023.
Sethna, J. P. & Kivelson, S. 1982 *Phys. Rev.* B **26**, 3513.
Shank, C. V., Yan, P., Fork, R. L., Orenstein, J. & Baker, G. L. 1982 *Phys. Rev. Lett.* **49**, 1660.
Su, W. P., Schrieffer, J. R. & Heeger, A. J. 1979 *Phys. Rev. Lett.* **42**, 1698.
Su, W. P., Schrieffer, J. R. & Heeger, A. J. 1980*a* *Phys. Rev.* B **22**, 2099.
Su, W. P. & Schrieffer, J. R. 1980*b* *Proc. natn. Acad. Sci. U.S.A.* **77**, 5626.
Su, Z. & Yu, L. 1983 *Phys. Rev.* B **27**, 5199.
Suzuki, N., Ozaki, M., Etemad, S., Heeger, A. J. & MacDiarmid, A. G. 1980 *Phys. Rev. Lett.* **45**, 1209.
Takayama, H., Lin-Lin, Y. R. & Maki, K. 1980 *Phys. Rev.* B **21**, 2388.
Tani, T., Grant, P. M., Gill, W. D., Street, G. B. & Clarke, T. C. 1980*a* *Solid St. Commun.* **33**, 499.
Tani, T., Grant, P. M., Gill, W. D., Street, G. B. & Clarke, T. C. 1980*b* *Synthetic Metals* **1**, 301.
Tomkiewicz, Y., Taranko, A. R. & Schultz, T. 1979 *Phys. Rev. Lett.* **43**, 1532.
Tomkiewicz, Y., Schultz, T., Brom, H. B., Taranko, A. R., Clarke, T. & Street, G. B. 1981 *Phys. Rev.* B **24**, 4348.
Vardeny, Z., Strait, J., Moses, D., Chung, T.-C. & Heeger, A. J. 1982 *Phys. Rev. Lett.* **49**, 1657.
Vardeny, Z., Orenstein, J. & Baker, G. L. 1983 *Phys. Rev. Lett.* **50**, 2032.
Weinberger, B. R., Ehrenfreund, E., Heeger, A. J. & MacDiarmid, A. G. 1980 *J. chem. Phys.* **72**, 4749.
Weinberger, B. R., Roxlo, C. B., Etemad, S., Baker, G. L. & Orenstein, J. 1984 *Phys. Rev. Lett.* **53**, 86.

Discussion

R. Pethig (*School of Electronic Engineering Science, University College of North Wales, Bangor, U.K.*). Have any dielectric measurements as a function of doping been made on polyacetylene? This might provide extra information on polarization phenomena.

A. J. Heeger. Measurements of the dielectric constant were made as a function of the dopant concentration by using infrared techniques (Hoffman 1982). A divergence in ϵ was observed as the concentration approached that of the semiconductor–metal transition.

Reference

Hoffman, D. M. 1982 Ph.D. thesis. University of Florida.

PHILOSOPHICAL TRANSACTIONS OF THE ROYAL SOCIETY A MATHEMATICAL, PHYSICAL & ENGINEERING SCIENCES